Simulation of short-chain polymer collapse with an explicit solvent

James M. Polson
Department of Physics, University of Prince Edward Island, 550 University Ave., Charlottetown, Prince Edward Island, C1A 4P3, Canada

Martin J. Zuckermann
Department of Physics, Simon Fraser University, Burnaby, British Columbia V5A 1S6, Canada

(Received 31 July 2001; accepted 5 February 2002)

We study the equilibrium behavior and dynamics of a polymer collapse transition for a system composed of a short Lennard-Jones (LJ) chain immersed in a LJ solvent for solvent densities in the range of $\rho=0.6$–0.9 (in LJ reduced units). The monomer hydrophobicity is quantified by a parameter $\lambda \in [0,1]$ which gives a measure of the strength of attraction between the monomers and solvent particles, and which is given by $\lambda=0$ for a purely repulsive interaction and $\lambda=1$ for a standard LJ interaction. A transition from the Flory coil to a molten globule is induced by increasing λ. Generally, the polymer size decreases with increasing solvent density for all λ. Polymer collapse is induced by changing the hydrophobicity parameter from $\lambda=0$ to $\lambda \geqslant 0.5$, where the polymer is in a molten globule state. The collapse rate increases monotonically with increasing hydrophobicity and decreases monotonically with increasing solvent density. Doubling the length of the chain from $N=20$ to $N=40$ monomers increases the collapse time roughly by a factor of 2, more or less independent of the hydrophobicity and solvent density. We also study the effect of conformational restrictions on polymer collapse using a chain model in which the bond angles are held near 109.5° using a stiff angular harmonic potential, but where free internal rotation is allowed, and find that the collapse times increase considerably with respect to the fully flexible polymer, roughly by a factor of 1.6–3.5. This increase is most pronounced for high solvent densities. © *2002 American Institute of Physics*. [DOI: 10.1063/1.1464819]

I. INTRODUCTION

The polymer collapse transition refers to the dramatic reduction in the average size of a single polymer chain in dilute solution when the solvent conditions are changed from "good" to "poor." First predicted by Stockmayer some 40 years ago,[1] and observed by Tanaka and co-workers over 20 years ago,[2,3] it remains a subject of much experimental, theoretical, and computational research today. An important reason for this intense interest lies in its close connection to protein folding, one of the most important unsolved problems in molecular biology,[4–6] in that the collapse of a homopolymer from a large coil to a compact globule is thought to be qualitatively similar to the initial stages of the protein folding process. A large majority of work on the polymer collapse transition has focused on the equilibrium properties of the transition, and, consequently, a detailed understanding of the relationship between equilibrium polymer size and solvent quality is now available.[7–9] On the other hand, a clear picture of the nature of the collapse dynamics has yet to emerge.

Theoretical studies of polymer collapse dynamics commenced with the phenomenological theory of de Gennes in 1985.[10] In this study, a two-stage collapse is proposed: first, the rapid formation of connected blobs of locally collapsed monomers along the initial contour of the chain, and, second, a slower process of lateral swelling and longitudinal contraction of the polymer with hydrodynamic friction until a roughly spherical globule is formed. A refined version of the theory was presented by Grosberg *et al.*[11] who recognized the importance of topological constraints. They argue the collapse proceeds through a different two-stage process, in which the polymer first collapses rapidly to form an unknotted, crumpled globule, where monomers proximal along the chain tend also to be proximal in space, and, second, relaxes slowly through quasiknotting to a more tangled state where monomers more distant on the chain are more likely to be close in space. More recent phenomenological theories by Halperin and Goldbart,[12] and by Klushin[13] present models in which the chain initially forms small collapsed clusters at random locations along the polymer backbone, which are connected by linear segments of monomers. The clusters accumulate monomers from these "bridges" until they become taut, after which the clusters are pulled together, until eventually they coalesce to form the final globule. Another approach was taken by Dawson and co-workers, who developed the Gaussian self-consistent method which is based on an analysis of the Langevin equation.[14–16] A three-stage collapse process was proposed, with specific scaling laws for each stage: first, the rapid formation of small collapsed globules; second, a coarsening stage in which blobs grow primarily by merging with smaller ones; third, a final relaxation phase characterized by compactification of internal structure and optimization of its surface. Another theory based on the Langevin equation was developed by Pitard and Orland[17] using a procedure originally developed for equilibrium dynamics by Edwards and co-workers. More recently, Pitard extended the method to include the effect of hydrodynamics

on the collapse dynamics.[18] Ganazzoli *et al*. have used a different analysis of the Langevin equation to study the collapse dynamics of a freely rotating chain.[19]

Experimental observation of polymer collapse dynamics is a challenging problem due to the strong coupling of the intrachain collapse with the interchain aggregation upon changing from good (or theta) solvent conditions to poor solvent conditions. However, recent developments in methodology have enabled the study of collapse dynamics in dilute solutions of noninteracting polymers in cases where the aggregation time is significantly longer than the collapse time.[20–24] In these studies, dynamic light scattering experiments are performed to monitor the size of the coil as a function of time upon quenching to poor solvent conditions by abruptly changing the temperature. Chu and co-workers were the first to report measurements of homopolymer collapse dynamics.[20,21] They observed a two-stage process in the collapse of polystyrene in cyclohexane. This was interpreted on the basis of a two-stage model for collapse proposed earlier.[10,11,25] Allegra and co-workers have challenged the interpretation of the results, suggesting instead that the second stage of kinetics actually corresponds to aggregation of small numbers of polymer chains which can have a hydrodynamic radius smaller than that of a single collapsed globule. Zhu and Napper[22] studied the collapse of poly (*N*-isopropylacrylamide) (PMMA) in water and interpreted their results in the context of the model of Dawson and co-workers.[14,15,26] The collapse times were found to vary inversely with the quench depth (i.e., the temperature difference between the theta and final quench states). In addition, the experimental results appear to be consistent with a two-stage collapse process, which is interpreted as corresponding to the final two stages of the predicted three-stage process, i.e., blob coarsening and globule compaction, though the validity of this interpretation was inconclusive. Nakata and Nakagawa[23] studied the collapse dynamics of poly(methyl methylacrylate) in isoamyl acetate, and found that the collapse proceeded in a single-stage process. In addition, the collapse time was observed to increase with increasing polymer chain length. Similar conclusions were reached by Kayaman *et al*.,[24] who studied the same polymer–solvent system. On the other hand, Kayaman *et al*. contend that the polymer collapse occurs much faster than that apparently measured by Nakata and Nakagawa. Further, they suggest that those authors had actually measured the much slower process of aggregation, essentially the same proposal by Allegra and co-workers in their interpretation of the results of Chu and co-workers.

Given the widely divergent pictures and scaling laws for polymer collapse presented the various theoretical studies, and the lack of consensus among experimentalists concerning even the basic interpretation of the observed data, let alone the ability to unambiguously test any of the various predicted scaling laws, a different approach to the problem would be useful. Over the past two decades or so, computer simulation has proven to be an effective bridge between theory and experiment in such cases. There have been a number of simulation studies of polymer collapse.[27–34] In some cases, these studies are useful to test the approximations and methodology of a theory which is built on a similar model as the simulations use. Dawson and co-workers, for example, employed dynamic Monte Carlo simulation methods to study collapse and observe results consistent with their theoretical predictions.[28] On the other hand, it is important to recognize that simulation results are at best only as good as the model employed. Each of the studies referenced above employs a model in which the effects of the solvent are incorporated in an implicit manner into effective pair interactions between monomers. The limitations of integrating out the solvent degrees of freedom to construct a pair potential as opposed to a many-body potential have been noted in, e.g., the equilibrium behavior of short oligomers.[35] As the dynamics of polymers are expected to be strongly affected by the solvent degrees of freedom through, e.g., hydrodynamic effects, there is no guarantee that the implicit-solvent collapse simulation results give even a qualitatively correct picture of polymer collapse.

Clearly, it is desirable to study polymer collapse using explicit-solvent simulation models to avoid the problems described above. To our knowledge, there have been only two such studies reported.[36,37] The paucity of such studies is due to the high computational cost of employing a necessarily large number of solvent particles in the simulations.

In our first study on this topic,[36] we studied a simple model system composed of a fully flexible polymer Lennard-Jones chain in a Lennard-Jones solvent. Both homopolymers and heteropolymers (random copolymers) were considered. To reduce the computational cost and to facilitate the study of chains of 100 or 200 monomers, we chose to model the system in two dimensions. In the case of the heteropolymers, we found that the collapse rates increase monotonically with increasing hydrophobicity. In addition, we observed that the collapse rates also generally decrease with solvent density in the range $\rho=0.5$–0.7 (in reduced Lennard-Jones units) though this density dependence was generally weaker for higher hydrophobicity and vanished in the limit of uniformly hydrophobic chains. For the case of homopolymers, we also found that the collapse rates increase with increasing hydrophobicity. We also compared the effect of hydrophobicity on collapse rates for homopolymers and heteropolymers, and found little difference between the collapse times, except at lower degrees of hydrophobicity. Finally, for random copolymers, we found no evidence of localized blobs formed along the chain during collapse, in contrast to various other simulation studies of implicit-solvent three-dimensional systems.

The second explicit-solvent simulation study of polymer collapse is the recent work of Chang and Yethiraj.[37] In this study, the direct role of the solvent in the collapse dynamics is investigated by carrying out a systematic comparison between equivalent implicit-solvent and explicit-solvent systems. The different systems are mapped onto one another by employing the polymer reference interaction site model (PRISM) theory[38,39] to calculate an effective monomer–monomer pair potential for the polymer–solvent model. They find that the collapse rate for the isolated polymer increases initially with increasing quench depth, but decreases with quench depth at later times. The latter feature was attributed to the trapping in local free energy minima along the

collapse pathway, an effect which is more pronounced with decreasing temperature. By contrast, the collapse rate for the polymer–solvent system increases uniformly at all times, in agreement with the results of our 2D study.[36] In addition, no trapping in intermediate states was observed. From these results, it was hypothesized that solvent "crowding" may assist a process like protein folding by smoothing out the free energy landscape.

In this study, we investigate polymer collapse dynamics in an explicit-solvent system, using essentially the same model and procedure used in Ref. 36, except that we now investigate a three-dimensional system and concentrate on homopolymers. Therefore, in this work, as in the previous study, the focus is on the investigation of the generic effects of varying the principal system properties on the equilibrium conformational behavior and the collapse dynamics of this model system, since the inclusion of solvent represents the correct physical picture. Hence, we do not carry out any simulations with an implicit-solvent model in the manner of Ref. 37 in order to understand the differences between the two classes of models on polymer collapse behavior. Specifically, we study the effects of hydrophobicity (which is controlled exclusively through the solvent–monomer interactions), solvent density and chain length on the collapse dynamics. We also study the effect of incorporating conformational restrictions on the dynamics by comparing the collapse dynamics of a chain with "fixed" bond angles and free internal rotation with those of the fully flexible chain model. An important aspect of this study is to investigate whether the results of the 2D study were general, or dimensionality related artifacts. As the 3D simulations are computationally costly, and we study the effects of several different parameters on collapse dynamics, we employ relatively small systems and short polymer chains. Of course, this limits the range of phenomena we can investigate, precluding, for example, testing the scaling predictions of different stages of collapse predicted by various theories. On the other hand, many important effects are already observable for such small systems, and the results should provide a useful means to guide similar studies of longer-chain systems which will be more feasible as computational speed improves.

II. MODEL AND METHODS

We consider a three-dimensional system composed of a single flexible polymer chain immersed in a Lennard-Jones (LJ) solvent. The solvent is a monomeric solvent in that the solvent particles have the same size and mass as the monomers on the polymer, although their respective interparticle interactions differ. Particle interactions are pairwise additive and depend on whether the particle is a monomer or a solvent particle. Solvent–solvent (SS) and monomer–monomer (MM) pair interactions are identical and given by a truncated and shifted 6-12 Lennard-Jones potential:

$$u_{\mathrm{MM}}(r)=u_{\mathrm{SS}}(r)=u_{\mathrm{LJ}}(r)-u_{\mathrm{LJ}}(r_C), r\leqslant r_C$$
$$=0, \quad r\geqslant r_C, \tag{1}$$

where

$$u_{\mathrm{LJ}}(r)=4\epsilon[(\sigma/r)^{12}-(\sigma/r)^{6}], \tag{2}$$

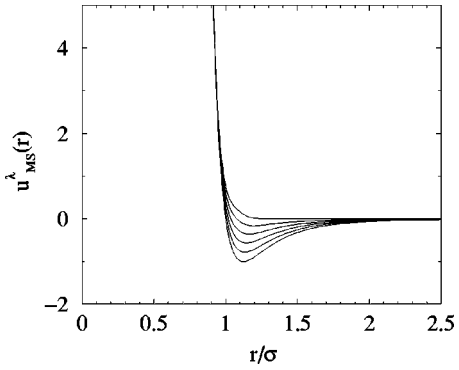

FIG. 1. Monomer–solvent pair potential $u^{\lambda}_{\mathrm{MS}}$ vs r, for hydrophobic interaction degree values $\lambda=1.0$, 0.8, 0.6, 0.4, 0.2, and 0.0 shown, respectively, from the top to the bottom.

where σ and ϵ are the usual LJ length and energy parameters, respectively. As well, we have chosen a cutoff distance of $r_C=2.5\sigma$. The monomer–solvent (MS) pair interaction has been designed to have the same repulsive-core size as the standard LJ interaction, but otherwise to have a potential well of variable depth. To this end, we first define a purely repulsive interaction, $u_{\mathrm{HS}}(r)$ between a "hydrophobic" (H) monomer and a solvent (S) particle:

$$u_{\mathrm{HS}}(r)=\omega(r)u_{\mathrm{LJ}}(r)+(1-\omega(r))u_{\mathrm{rep}}(r). \tag{3}$$

Here $u_{\mathrm{rep}}(r)$ is a steeply repulsive interaction given by $u_{\mathrm{rep}}(r)=4\epsilon(r/\sigma)^n$, where we have chosen the value $n=30$. The function $\omega(r)$ is a weighting function which has the effect of transforming $u_{\mathrm{HS}}(r)$ from values close to $u_{\mathrm{LJ}}(r)$ at low r to values close to $u_{\mathrm{rep}}(r)$ at larger r in such a way as to avoid the presence of an attractive well. To this end we choose $\omega(r)$ to be a displaced error function

$$\omega(r)=(1+\mathrm{erf}((a-r)/\sqrt{2}\gamma))/2, \tag{4}$$

where $a=1.035$ and $\gamma=0.040$. We also define a "hydrophilic" (P) monomer as one that interacts with a solvent particle via the modified LJ interaction of Eq. (1): $u_{\mathrm{PS}}(r)=u_{\mathrm{SS}}(r)=u_{\mathrm{MM}}(r)$. The general monomer–solvent pair potential $u^{\lambda}_{\mathrm{MS}}(r)$ is a linear combination of $u_{\mathrm{HS}}(r)$ and $u_{\mathrm{PS}}(r)$:

$$u^{\lambda}_{\mathrm{MS}}(r)=\lambda u_{\mathrm{HS}}(r)+(1-\lambda)u_{\mathrm{PS}}(r), \tag{5}$$

where the degree of hydrophobicity, λ, ranges from 0, in which case $u^{\lambda}_{\mathrm{MS}}(r)=u_{\mathrm{PS}}(r)$, the hydrophilic limit, to 1, in which case $u^{\lambda}_{\mathrm{MS}}(r)=u_{\mathrm{HS}}(r)$, the hydrophobic limit. The potential $u^{\lambda}_{\mathrm{MS}}(r)$ is illustrated in Fig. 1 for several values of λ.

In addition to the interactions between nonbonded particles described above, we include the following bond-stretching and bond angle-bending potentials. Adjacent monomers on the chain are bonded by stiff springs which interact with a potential

$$u_b(r)=(k_b/2)(r-l_b)^2, \tag{6}$$

where we have chosen the spring constant of $k_b=5000\epsilon\sigma^{-2}$ and a bond length of $l_b=\sigma$. Any adjacent pair of bonds on the polymer with a relative orientation of angle of θ contributes the following to the total potential energy:

$$u_\theta(r)=(k_\theta/2)(\theta-\theta_0)^2. \tag{7}$$

In most of the simulations, we have considered "fully flexible" (i.e., freely jointed) chains for which $k_\theta=0$. In certain cases, we have studied the effects of conformational restrictions on the chains by employing this potential with values of $k_\theta\sigma^2/\epsilon=50$ and $\theta_0=109.5°$. This value of k_θ essentially fixes the bond angle θ to within a degree or two of θ_0 at the temperatures considered in this study. In effect we are employing a model with free internal rotation and a "fixed" bond angle. We employ such a stiff harmonic angular potential rather than a true bond angle constraint, as the latter is somewhat more cumbersome to use in MD simulations. In this study, we refer to these conformationally restricted chains as "semi-flexible" chains. However, this is not meant to imply that the chains are characterized by a persistence length that is much greater than the bond length. For the value of θ_0 employed, we expect that the correlations in bond angle direction to become insignificant over just a few bond lengths. On the other hand, the angular restrictions do have a significant impact on equilibrium conformational statistics and collapse dynamics.

All quantities described below are expressed in Lennard-Jones reduced units. Specifically, distances are expressed in terms of σ, energies in terms of ϵ, temperature in terms of k_B/ϵ, where k_B is Boltzmann's constant, and time in terms of $\sqrt{m\sigma^2/\epsilon}$, where m is the mass of the each solvent particle and monomer. Further, the density of the system is defined to be the total particle number density, $\rho=(N+N_s)\sigma^3/V$.

To permit an efficient calculation of the pair potentials described by Eqs. (3) and (5) and their corresponding pair forces, we employed a lookup table using 20 000 values of r for $0.5\leqslant r\leqslant r_C$. Further, we employed the Verlet neighbor list method[40] for calculation of all pair forces.

Simulations performed to monitor the equilibrium properties of the system employed the constant-temperature, constant-volume (NVT) ensemble at a temperature of $T=1.0$ with a Nosé–Hoover thermostat to regulate the temperature. The corresponding equations of motion were integrated using the reversible time-propagation integrators described by Martyna *et al.*[41] In most cases we used a time step of $\delta t=0.005$, and a thermostat frequency of $\omega_p=5.0$, from which the thermostat mass is given by $Q_p=N_f k_B T/\omega_p^2$, where N_f is the number of degrees of freedom of the system.[41] In addition, we employed the reference system propagator (RESPA) multiple time step (MTS) method to improve energy conservation.[41–43] This enabled us to use a relatively large time step despite the presence of stiff bonds between adjacent monomers, and the stiff bond angle-bending interaction. Using the bonding force (and, in cases where $k_\theta\neq 0$, the angle-bending force) as the reference force, and employing a short time step of $\delta t_s=0.001$ (i.e., $n_s\equiv\delta t/\delta t_s=5$ reference force calculations per large time step) we observe satisfactory energy conservation.[44]

Most simulations employed polymers of length $N=20$ monomers immersed in a bath of N_s solvent particles, such that the total number of particles was $N+N_s=1000$. In a few cases, we considered larger systems with $N=40$ monomers and $N+N_s=3000$ particles. For any particular density, the monomers and solvent particles were initially placed on a cubic lattice. For convenience, the initial polymer chain conformation was composed of straight parallel segments along one face of the simulation cell with sharp bends at the periodic boundaries. The system was next equilibrated for a considerable time, $\Delta t\geqslant 10\,000$, before any measurements were taken. The system coordinates were then used as initial coordinates for subsequent calculations. Upon variation of some system parameter (e.g., λ), statistics would be accumulated for $\Delta t=1000$–$96\,000$. Longer run times were required for systems with high solvent density, and, especially, for small λ (i.e., good solvent conditions, in which the chain is in the coil state). After each simulation, the final configuration was used as the initial configuration for a simulation with next value of the parameter, and so on. Prior to each accumulation of statistics, the system was further equilibrated for a period of at least $\Delta t=200$.

Many of the simulations in this study were performed to measure the collapse dynamics of the polymer upon abruptly changing the conditions of the system. To induce collapse, we follow the approach taken in Ref. 36, in which equilibrium configurations for a $\lambda=0$ (hydrophilic) homopolymer in the Flory coil state are used as prequench initial configurations. Quenches are performed by changing the solvent–monomer interactions. In most cases, this is accomplished by changing the MS interaction parameter λ from 0 to a higher (more hydrophobic) value for which the polymer prefers to be in the collapsed state. Note that the collapsed state of the polymer chain is a liquidlike globule at the temperature employed, $T=1.0$, and the range of solvent densities considered, as was the case in our earlier 2D study.[36]

In order to obtain reliable statistics from the quenches, it was necessary to use at least 100 initial configurations. The configurations were generated by conducting a very long simulation, and saving the coordinates after every time interval of at least $\Delta t=100$. Each quench was carried out over a time interval of $\Delta t=100$ in most cases, and $\Delta t=500$ for the cases of long chains and semiflexible chains. During each quench, we employed the constant energy (NVE) simulation method to avoid the artificial dynamics associated with the Nosé–Hoover thermostat. Note that in changing the nature of the interactions during the quench while keeping the energy fixed to that of the prequench state, we expect that the temperature during the collapse to differ from that associated with the initial configuration. However, we find that at the temperature considered, $T=1.0$, and for the system sizes we investigated, the average temperature during the collapse is a negligible 1–2% higher than its initial value.

In this study, two key quantities were measured and used as descriptors of the state of the polymer chain. The first is the radius of gyration, R_g, which is given by its standard definition

$$R_g^2=N^{-1}\left\langle \sum_{i=1}^{N} |\vec{R}_i-\vec{R}_{\mathrm{CM}}|^2 \right\rangle, \tag{8}$$

where $\vec{R}_i$ is the position of the ith monomer, $\vec{R}_{\mathrm{CM}}$ is the center of mass of the polymer chain, and where the average $\langle\cdots\rangle$ denotes a time (or ensemble) average over all configurations of the chain. The second measure is n_{MM}, the aver-

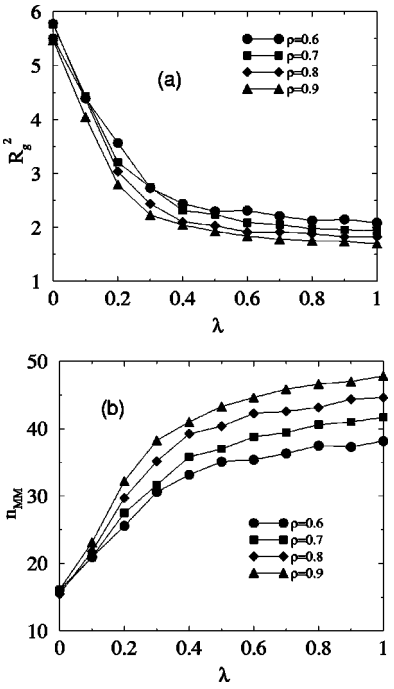

FIG. 2. Radius of gyration squared R_g^2 (a) and number of monomer–monomer contacts n_{MM} (b) vs degree of hydrophobicity λ for a homopolymer of length $N=20$ at $T=1.0$ at densities $\rho=0.6$, 0.7, 0.8, and 0.9.

age number of monomer–monomer contacts, where in this case a contact is defined as two nonbonded monomers separated by a distance $r \leqslant 1.5\sigma$.

Finally, the rate of collapse was quantified by defining two separate collapse times t_{50} and t_{90} for monitoring both $R_g^2(t)$ and $n_{\mathrm{MM}}(t)$. t_{50} is defined as the average time taken for either R_g^2 or n_{MM} to decay or grow from its initial value by 50% of the difference between the initial and final values. Likewise, t_{90} is defined as the average time taken for either R_g^2 or n_{MM} to decay or grow from its initial value by 90% of the difference between the initial and final values.

III. RESULTS AND DISCUSSION

A. Equilibrium properties

The dependence of the equilibrium averages of R_g^2, and n_{MM} on the monomer–solvent coupling parameter, λ, for a homopolymer of length $N=20$ is illustrated in Figs. 2(a) and 2(b), respectively. Generally, we observe a decrease in the size of the homopolymer chain with increasing λ, as evidenced by both the decrease in R_g^2 and the increase in n_{MM}. The change in R_g^2 and n_{MM} are both greatest in the range $\lambda \in [0,0.5]$, and considerably less so for $\lambda \in [0.5,1]$. In fact, R_g^2 is almost constant in the latter range. In this regime, the homopolymer is in a liquidlike "globule" state characterized by a size whose lower limit is determined the short-range repulsive component of the monomer–monomer LJ interaction. Generally, we also observe a slight decrease of the spatial extent of the polymer, i.e., a decrease in R_g^2 and an increase in n_{MM}, with increasing solvent density ρ. This is especially clear for higher λ, though less so for low λ where large fluctuations in these quantities create considerably larger uncertainties. Finally, the small shift of the transition to lower λ with increasing ρ suggests that increasing solvent density stabilizes the collapsed state.

The origin of the λ behavior of R_g^2 and n_{MM} is straightforward, and follows from a consideration of the Helmholtz free energy, $F \equiv E - TS$, where E is the total energy and S is the total entropy of the polymer–solvent system. The conformational entropy of the polymer chain is greater when the chain is in the conformationally extensive Flory coil state, than when it is in the conformationally compact globule state. On the other hand, the translational entropy associated with the solvent particles is probably lower when the polymer is in the coil state than when it is in the globule state. In athermal systems (hard-particle chains immersed in hard-particle solvents), the competition between these two entropies can lead to a polymer collapse transition driven by an increase in solvent density,[45–52] though this transition has never been observed in simulations of off-lattice additive-potential hard-core model systems, where the polymer is always observed in the coil state.[53] By analogy, in the present case, we expect that the Flory coil is entropically favored over the globule state.

The relationship of the potential energy to the conformational size of the polymer chain depends on both the solvent density and monomer–solvent interaction parameter λ. In the limit of $\rho \to 0$, the potential energy is determined completely by the monomer–monomer interactions; thus, the energy will be minimized roughly when the number of contacts between monomers is maximized, a situation realized when the chain is in the collapsed state. In this limit, a collapse transition can be driven by changes in the temperature, T, which controls the relative importance of the energy and the entropy to the free energy. Simulation studies of the collapse transitions of this type of model have been widely reported. On the other hand, the present situation is complicated by the presence of the solvent particles, which also interact with the monomers with attractive interactions with a magnitude determined by λ. At the relatively high densities considered here ($\rho \in [0.6,0.9]$), the monomers maintain a relatively high number of contacts with solvent particles, which means that for low λ, the globule state is no longer be energetically favorable with respect to the coil state.

To illustrate this point, we analyze the correlations in the distributions of n_{MM}, and the contact potential energy U_{con} (defined as the sum of the contributions to the potential energy from all MM, MS, and SS interactions) at different values of λ. Specifically, we consider a system at a solvent density $\rho=0.9$ at $\lambda=0$, 0.1, 0.2 0.3, 0.4, and 0.6. Figure 3 shows the average U_{con} (calculated for a narrow range of $\Delta n_{\mathrm{MM}}=2.0$ for $\lambda=0$, 0.1, 0.2, 0.3, and 0.4, and $\Delta n_{\mathrm{MM}}=4.0$ for $\lambda=0.4$ and 0.6) versus n_{MM}. At $\lambda=0$, U_{con} is independent of n_{MM}; thus, the total energy is independent of the polymer size, in agreement with our statement above regarding the Flory chain limit. Consequently, the coil state will be favored due to the importance of the configurational entropy to the free energy. However, as λ decreases, i.e., when the contact potential energy between monomers and neighboring solvent particles decreases, it becomes increasingly more energetically favorable for the chain to be in a high-n_{MM} state,

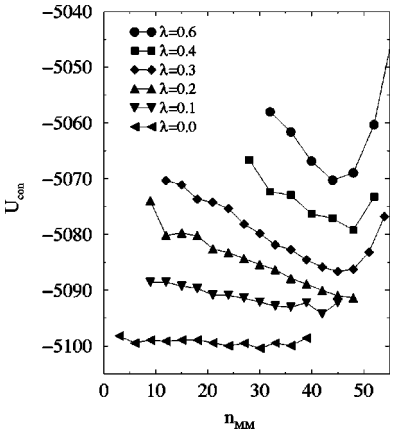

FIG. 3. Total average contact potential energy U_{con} (see text for definition) vs monomer–monomer contact number n_{MM} for a homopolymer of length $N=20$ in a solvent of density $\rho=0.9$ and at a temperature $T=1.0$. Note that curves are actually spaced further apart than shown in this figure. We have added the following energy shifts to the data to provide a more expanded energy axis in the figure: $\Delta U_{\mathrm{con}}=0$, -10, -20, -30, -35, and -50 for $\lambda=0.0$, 0.1, 0.2, 0.3, 0.4, and 0.6, respectively.

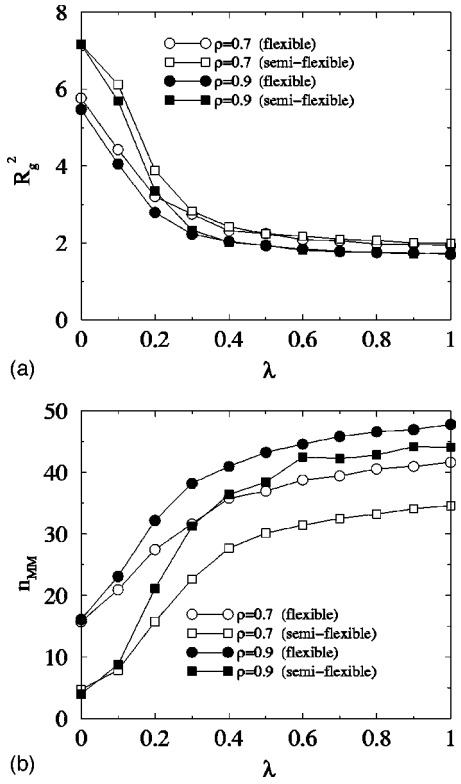

FIG. 4. Radius of gyration squared R_g^2 (a) and number of monomer–monomer contacts n_{MM} (b) vs degree of hydrophobicity λ for flexible and semiflexible homopolymers for a chain of length $N=20$ at $T=1.0$ at densities $\rho=0.7$ and 0.9.

i.e., a more compressed state. Eventually, the energy dominates the free energy, and the chain collapses to a globule. Thus, increasing λ drives a polymer collapse transition.

A qualitative understanding of solvent-density dependence of R_g^2 and n_{MM} is also straightforward, and follows from a consideration of the translational entropy of the solvent. In an earlier study, Escobedo *et al.*[54] investigated an athermal system composed of a fused hard-sphere flexible chain in a hard sphere solvent. In that case, the polymer size was also observed to decrease with increasing solvent density, an effect that is due to the fact that the free volume accessible to the solvent particles increases when the polymer decreases. This effect becomes more pronounced with increasing solvent density. As the hard-sphere type model is a reasonable approximation of the repulsive component of the LJ potential, it is not surprising to observe this effect in the present case.

The λ dependence of R_g^2 and n_{MM} is qualitatively consistent with our previous results for a two-dimensional homopolymer–solvent composite system. Evidently the dimensionality of the model system results is not a principal factor affecting the thermodynamics of the collapse transition.

Figure 4 illustrates the effect introducing the angular constraints to the polymer chain on the conformational size. The results for both R_g and n_{MM} show that, for all densities considered (data for $\rho=0.6$ and 0.8 are not shown), the semiflexible chains are more conformationally extended in good solvent conditions at low λ. On the other hand, for $\lambda \geqslant 0.3$, the flexible and semiflexible chains have essentially the same R_g, suggesting that polymer globules are approximately the same size. Of course, this result is expected to be highly sensitive to the value of θ_0: for higher values, the semiflexible chains are expected assume a more conformationally extended toroidal structure, as opposed to a compact spherical globule, in the collapsed state, as has been observed in other semiflexible model systems with a high degree of chain stiffness.[55–58] It is also interesting to note that the contact number n_{MM} is noticeably different in the flexible and semiflexible cases in contrast to R_g. Finally, we note that increasing density has a comparable degree of effect in decreasing R_g and increasing n_{MM} in the flexible and semi-flexible chain systems.

B. Collapse dynamics

Figure 5 shows the time dependence of R_g^2 and n_{MM} following a quench for a homopolymer of length $N=20$ in a solvent of density $\rho=0.7$. Each overlaid curve corresponds to a different post-quench value of λ. In addition, each curve represents an average over at least 100 initial configurations. Clearly, the collapse rate increases with increasing λ, that is, with increasing monomer hydrophobicity.

In order to provide a more quantitative description of the relationship between the collapse rate and the degree of hydrophobicity, we use the following approach. The average curves are fit to a stretched exponential of the form

$$R_g^2(t)=a_0 e^{-(t/\tau)^{\beta}}-a_1 \tag{9}$$

for the radius of gyration, and

$$n_{\mathrm{MM}}(t)=a_0(1-e^{-(t/\tau)^{\beta}})-a_1 \tag{10}$$

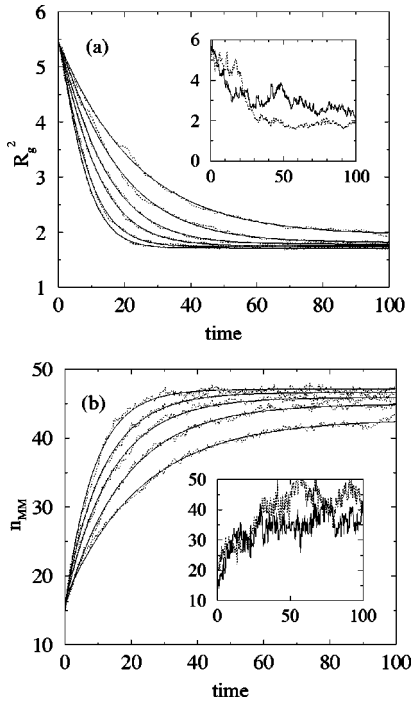

FIG. 5. Plots of (a) radius of gyration squared R_g^2 vs time, and (b) number of monomer–monomer contacts n_{MM} vs time, for homopolymer collapse for homopolymer chains of length $N=20$ monomers in a solvent of density $\rho=0.7$ and temperature $T=1.0$. The curves correspond to degrees of hydrophobicity $\lambda=0.5, 0.6, 0.7, 0.8, 0.9, 1.0$, from top to bottom for (a), and from bottom to top for (b). Insets show two sample single quenches at $\lambda=0.5$. Polymer collapse is induced by switching the hydrophobic interaction parameter from $\lambda=0$ to the value labeled above. The temperature is fixed to $T=1.0$.

for the monomer–monomer contact number. Note that the parameters a_0 and a_1 are simply related to the equilibrium average of R_g^2 and n_{MM} for the prequench and post-quench values of λ, while the time constant τ and the exponent β are the quantities which relate directly to the dynamics. These functional forms generally provided very good quality fits for all decay curves analyzed, although it should be stressed that there is no *a priori* theoretical argument that R_g^2 and n_{MM} should conform to Eqs. (9) and (10). Consequently, we choose not to focus on the fit values of τ and β. Instead, the best-fit curves are used to determine the collapse times t_{50} and t_{90}, the 50% and 90% decay times defined in Sec. II.

The collapse times t_{50} and t_{90} are plotted as a function of the post-quench degree of hydrophobicity λ in Figs. 6 and 7, respectively, for solvent densities of $\rho = 0.6, 0.7, 0.8$ and 0.9. For each density, both t_{50} and t_{90} decrease monotonically with increasing λ. The λ dependence of the collapse times determined from $R_g^2(t)$ are qualitatively consistent with those determined from $n_{\mathrm{MM}}(t)$, though the t_{50} determined from the $R_g^2(t)$ are consistently greater than those determined by the $n_{\mathrm{MM}}(t)$ by $\Delta t=0.5$–1, while the t_{90} determined from the $R_g^2(t)$ are consistently less than those determined by the $n_{\mathrm{MM}}(t)$ by $\Delta t=1$–2.

Figures 6 and 7, also show that the collapse times monotonically *increase* with increasing solvent density for the full range of post-quench λ considered here. However, the ρ dependence of the collapse times is clearly not linear; rather,

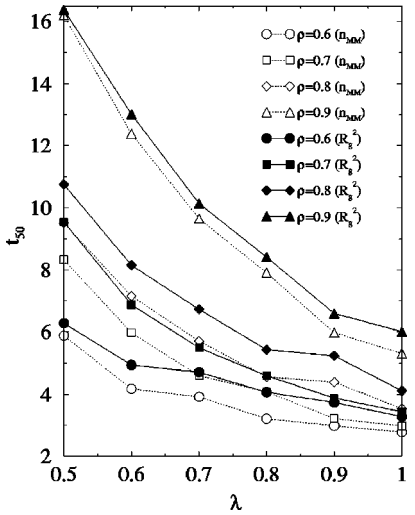

FIG. 6. Collapse time t_{50} (see text for definition) vs λ for homopolymer chains of length $N=20$ monomers in a solvent with $N_{\mathrm{tot}}=N+N_s=1000$, where N_{tot}, N, and N_s are the total number of particles, the number of monomers, and the number of solvent particles, respectively. Polymer collapse at $T=1.0$ is induced by switching the hydrophobic interaction parameter from $\lambda=0.0$ to the value labeled on the horizontal axis in the figure. The collapse times have been determined by monitoring the decay of the radius of gyration squared, R_g^2 (filled symbols) and the number of monomer–monomer contacts, n_{MM} (open symbols).

the rate of increase of t_{50} and t_{90} with ρ increases as the density increases.

The λ dependence of the collapse times presented in Figs. 6 and 7 are qualitatively consistent with the results from our previous 2D study.[36] Note, however, that we did not consider the combined effects of hydrophobicity and solvent density on homopolymers in that study. However, at the low densities considered ($\rho=0.5$ and 0.7), the collapse rates for $\lambda=1$ homopolymers were ρ independent. We note that this is also true at low solvent density ($\rho=0.6$ and 0.7) in the

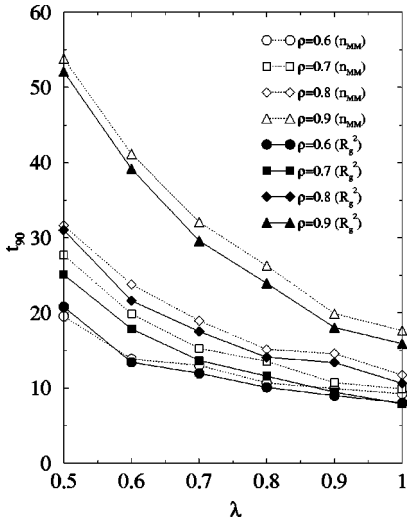

FIG. 7. Collapse time t_{90} (see text for definition) vs λ for the same system as described in the figure caption of Fig. 6. The collapse times have been determined by monitoring the decay of the radius of gyration squared, R_g^2 (filled symbols) and the number of monomer–monomer contacts, n_{MM} (open symbols).

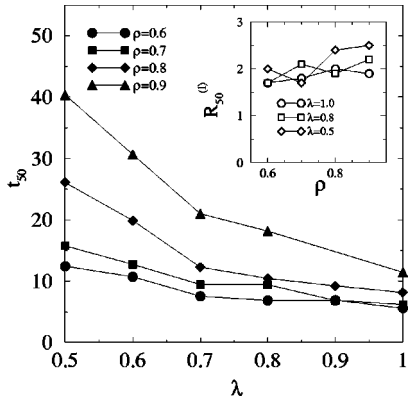

FIG. 8. Collapse times t_{50} vs λ for a homopolymer–solvent system for polymer length of $N=40$. The inset shows $R_{50}^{(l)}$ (the ratio of t_{50} for $N=40$ to t_{50} for $N=20$) vs solvent density ρ for $\lambda=1$, 0.8, and 0.5.

present study for $\lambda=1$ homopolymers. Thus, the current results are consistent with those of the 2D study. As well, the increasing divergence of the collapse times in Figs. 6 and 7 with decreasing λ is qualitatively similar to the trend for random copolymers with increasing hydrophobicity in 2D in Ref. 36. As the homopolymer collapse times at one density ($\rho=0.7$) were virtually identical to those of the copolymer for most of the range of hydrophobicity considered, it is quite likely that the ρ dependence of the collapse times observed in 3D would follow the same trends in 2D. Thus, we argue that, as is the case for the equilibrium properties studied, the dimensionality of the system does not strongly affect the qualitative relationship of the collapse rates to quench depth and solvent density.

The monotonic decrease in collapse times with increasing quench depth (in this case, governed by the post-quench value of λ) is also consistent with the explicit-solvent simulation results of Chang and Yethiraj.[37] Note that these results were found to differ considerably from the implicit-solvent simulation results of that same study, for which it is observed that increasing the quench depth leads to a more rapid collapse only at short times, but a considerably slower collapse at longer times. We have demonstrated here that this result is independent of solvent density for LJ-type model systems. Finally, we also note that the relationship between collapse rate and quench depth is consistent with the experimental results of Zhu and Napper for the PMMA in water.[22]

The uniform decrease in the collapse rates with increasing solvent density ρ is a significant result which deserves some comment. On the one hand, it is clear that increasing the solvent density will increase the viscosity of the fluid as well as increase the drag on the monomers as the chain collapses. Based on these considerations, a slower collapse would be expected. Kuznetsov *et al.*, for example, observed a similar increase in collapse times with increasing solvent viscosity in an analysis of the collapse dynamics of a homopolymer using the Gaussian self-consistent method.[16] However, it is also likely that the coil-globule free energy difference increases with increasing solvent density. For example, for $\rho=0.7$ and 0.9 we find that the difference in the average energy per particle $\Delta E(\rho)\equiv(E_{\lambda=1}-E_{\lambda=0})/N$ is $\Delta E(\rho=0.7)=-0.06$ and $\Delta E(\rho=0.9)=-0.12$. Thus, from energy considerations alone, the quench is driven more strongly at higher solvent densities. (Of course, it is not clear how the coil-globule entropy difference in an explicit-solvent system depends on solvent density.) From this argument, it could be expected that the collapse rate increases with increasing ρ, at least over some range of ρ and λ. Clearly, the former effect wins out over the latter. It would be interesting to know to what extent these results depend on the microscopic properties of the solvent, for example, the monomer/solvent size ratio.

TABLE I. Effect of polymer chain length and chain stiffness on the collapse times t_{50} and t_{90} (see text for definition). $R_{50}^{(l)}$ and $R_{90}^{(l)}$ are the ratio of the t_{50} and t_{90} collapse times respectively, for chains of length $N=40$ with respect to chains of length $N=20$. $R_{50}^{(s)}$ and $R_{90}^{(s)}$ are the ratio of the t_{50} and t_{90} collapse times, respectively, for semiflexible chains of length $N=20$ with respect to fully flexible chains of the same length.

ρ	λ	$R_{50}^{(l)}$	$R_{90}^{(l)}$	$R_{50}^{(s)}$	$R_{90}^{(s)}$
0.6	1.0	1.7	1.7	1.6	1.5
0.6	0.9	1.8	1.8	1.6	1.3
0.6	0.8	1.7	1.6	1.6	1.5
0.6	0.7	1.6	1.7	1.6	1.5
0.6	0.6	2.2	2.0	1.9	1.7
0.6	0.5	2.0	1.6	1.9	1.4
0.7	1.0	1.8	1.9	1.5	1.5
0.7	0.9	1.8	1.7	1.7	1.8
0.7	0.8	2.1	2.0	1.8	1.8
0.7	0.7	1.7	1.9	1.8	2.0
0.7	0.6	1.9	1.9	1.8	1.9
0.7	0.5	1.7	1.8	1.9	1.8
0.8	1.0	2.0	2.0	2.1	1.9
0.8	0.9	1.8	2.0	1.9	1.8
0.8	0.8	1.9	2.0	2.1	2.0
0.8	0.7	1.8	1.9	2.3	2.2
0.8	0.6	2.4	2.7	2.2	2.2
0.8	0.5	2.4	2.0	2.7	2.2
0.9	1.0	1.9	2.0	2.9	2.8
0.9	0.9	2.3	2.1	3.3	3.2
0.9	0.8	2.2	2.0	3.2	2.7
0.9	0.7	2.1	1.9	3.2	2.8
0.9	0.6	2.4	2.1	2.9	2.4
0.9	0.5	2.5	2.1	3.5	3.0

We now consider briefly the effect of increasing chain length on the rate of polymer collapse. Figure 8 shows the collapse time t_{50} [determined from an analysis of $R_g^2(t)$] versus λ at $\rho=0.6$, 0.7, 0.8, and 0.9 for a homopolymer chain of length $N=40$. [The λ dependence of t_{90}, as well as the t_{50} and t_{90} determined from an analysis of $n_{\mathrm{MM}}(t)$ yielded comparable results; consequently, we choose not to show those results.] The overall trend is the same as for the $N=20$ chain: the collapse time decreases monotonically with increasing λ, and increases monotonically, though in the same nonlinear manner as previously, with increasing solvent density. The one clear difference is quantitative: t_{50} is considerably longer for the $N=40$ chain.

The effect of increasing the polymer chain length on the collapse times is quantified in Table I. We define the quantity $R_{50}^{(l)}$ as the ratio of the collapse time t_{50} for the $N=40$ chain to that of the $N=20$ chain, and, likewise, $R_{90}^{(l)}$ as the same

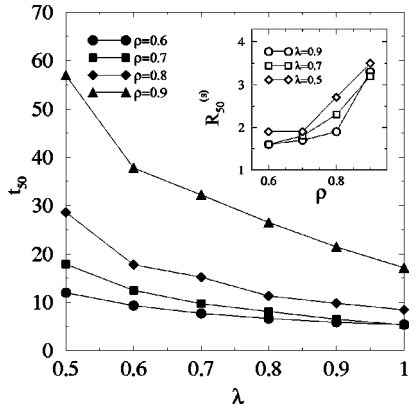

FIG. 9. Collapse times t_{50} vs λ for a homopolymer–solvent system for a semiflexible polymer of length $N=20$. The inset shows $R_{50}^{(s)}$ (the ratio of t_{50} for $N=40$ to t_{50} for $N=20$) vs solvent density ρ for $\lambda=0.9$, 0.7, and 0.5.

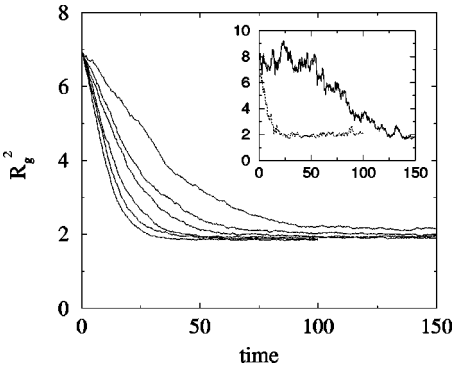

FIG. 10. R_g^2 vs time for a semiflexible polymer length of $N=20$ in a solvent of density $\rho=0.8$. From top to bottom, the curves correspond to post-quench hydrophobicity values of $\lambda=0.5$, 0.6, 0.7, 0.8, 0.9, and 1.0. The inset shows typical collapse curves of single-collapse events for $\lambda=0.5$ (top) and 1.0 (bottom).

ratio for the t_{90} collapse time. From the table, it is clear that doubling the length of the chain from $N=20$ to $N=40$ approximately doubles the collapse times. There is no consistent change in $R_{50}^{(l)}$ and $R_{90}^{(l)}$ with the post-quench λ, though there might be a slight increase in these ratios with increasing solvent density. The ρ dependence of $R_{50}^{(l)}$ for $\lambda=0.5, 0.8$, and 1.0 is illustrated in the inset of Fig. 8.

The increase in the collapse times with increasing chain length is an expected result which is consistent with other simulation studies using both implicit-solvent[27,28] and explicit-solvent[37] models, as well as with experiment.[22] The present study demonstrates that the factor by which the collapse times increase is not sensitive to the quench depth or the solvent density for relatively short chains. It remains to be seen how consistent these findings are for significantly longer chains.

Next, we examine the effect of chain stiffness on the homopolymer collapse dynamics. Figure 9 shows the collapse time t_{50} as a function of the post-quench λ for a chain of length $N=20$ for solvent densities of $\rho=0.6$, 0.7, 0.8, and 0.9. The collapse time t_{50} was determined from an analysis of $R_g^2(t)$. The data for t_{90} and for the collapse times determined from an analysis of $n_{\mathrm{MM}}(t)$ were qualitatively similar (data not shown). A comparison of Figs. 6 and 9, shows that the same general trends for the semiflexible chain are observed as in the case of the fully flexible chain. Specifically, the collapse time decreases monotonically with increasing λ, and increases monotonically with increasing solvent density. However, the collapse times are consistently larger for the semiflexible chain system. To quantify this effect, we define the quantity $R_{50}^{(s)}$ as the ratio of the collapse time t_{50} for the semiflexible chain relative to that of the fully flexible chain, and $R_{90}^{(s)}$ as the same ratio for the t_{90} collapse time. These ratios are also presented in Table I. Clearly, there is no significant variation of either ratio with the post-quench λ, though there may be a slight increase in the collapse times with λ. On the other hand, there is a significant increase in the ratios with increasing density. This effect is particularly noticeable at the highest density considered, $\rho=0.9$, where the ratio is roughly double that at $\rho=0.6$. This marked increase in $R_{50}^{(s)}$ with ρ for $\lambda=0.5$, 0.7, and 0.9 is illustrated in the inset to Fig. 9. Evidently, an increase in solvent density has a considerably stronger effect on the slowing down the collapse dynamics of a conformationally restricted polymer chain than for a fully flexible polymer chain.

Ganazzoli *et al.*[19] have studied the collapse kinetics of a freely rotating chain using an approximation of the Langevin equation. They examined chains of length $N=10$, 20, and 40 with a bond angle of $\theta_0=\cos^{-1}(-1/e)=111.6°$, close to the value of 109.5° considered here. They observe a two-stage decay in R_g upon quenching: a rapid collapse stage followed by a long time interval (the "induction time") during which the chain size is almost constant, which in turn is followed by a rapid final contraction to the collapsed globule. The induction time and the reduction in chain size during the second stage of collapse are found to decrease and increase, respectively, with increasing quench depth. On the other hand, our simulation results show no evidence for this behavior for chains of length $N=20$. Figure 10 shows the time dependence of R_g^2 for a semiflexible polymer in a solvent of density $\rho=0.8$ for various post-quench values of λ. The results are qualitatively similar to results at other ρ. In each case, there is no evidence of two rapid collapse stages separated by a time of near-constant polymer size. This is also true for single-event collapse curves, in addition to the ensemble-averaged collapse curves, as illustrated in the insert of the figure. It could be possible that the quenches considered here are not deep enough to make the effect appreciable enough to be measured, or that the fact that the bond lengths and angles are not rigidly fixed allows an easier relaxation to the globule without requiring such a high degree of cooperativity between the internal modes, as was observed by Ganazzoli *et al.*[19] On the other hand, it is also possible that the approximations employed in the theory have exaggerated the importance of the effect. Further studies will be required to resolve this issue.

IV. CONCLUSIONS

We have studied the equilibrium properties and the collapse dynamics of a single homopolymer chain in an explicit monomeric Lennard-Jones solvent. An advantage of such an approach is that the degree of hydrophobicity of monomers

is governed directly by the monomer–solvent interaction, rather than by effective pair interactions between monomers. Thus, the explicit-solvent approach provides a more realistic microscopic description of hydrophobicity. In our model, more hydrophilic monomers had a higher degree monomer–solvent attraction while the monomer–solvent pair potential for hydrophobic monomers consisted only of a short-range repulsive interaction. A transition from a conformationally extended Flory coil to a compact globule was observed upon increasing the monomer hydrophobicity. At low λ, the coil phase is not energetically favored over the globule phase, but is stable because of a higher entropy of this state of the polymer–solvent system. At high λ, the globule phase is stable because it minimizes monomer–solvent contacts and maximizes monomer–monomer and solvent–solvent attractions, and thus is considerably more energetically favorable. Increasing the solvent density leads to an overall decrease in the size of the polymer over the full range of hydrophobicity considered (although statistical fluctuations were too large to confirm this at $\lambda=0$), and has the effect of stabilizing the globule phase by shifting the transition to lower λ. We argue that this effect is entropic in nature, having been observed in various athermal polymer–solvent systems.

We studied the combined effects of quench depth, solvent density, chain length, and conformational restrictions on the polymer collapse dynamics. The collapse was induced by instantaneously changing the hydrophobicity from $\lambda=0$ (the hydrophilic limit) to values $\lambda\geqslant 0.5$. Generally, we find that the collapse rate increases monotonically with increasing quench depth at both short and long times. This result is consistent with the explicit-solvent simulation results of Chang and Yethiraj.[37] We find that the collapse rates decrease monotonically with increasing solvent density at all quench depths. The rate of decrease is not constant, but rather increases with increasing density. Doubling the chain length from $N=20$ to $N=40$ increases the collapse time by roughly a factor of 2, more or less independent of the solvent density or quench depth. The collapse times for a semiflexible polymer, constructed by keeping the bond angles close to $\theta_0=109.5°$ but allowing free internal rotation, were also longer than the freely jointed flexible polymer. In this case, however, the effect depended strongly on the solvent density: the ratio of the collapse time of the semiflexible chain to that of the fully flexible chain ranged from 1.6 at $\rho=0.6$ to 3.5 at $\rho=0.9$. Finally, we did not observe a two-stage collapse for the semi-flexible polymer as predicted in the theoretical work of Ganazzoli *et al*.[19]

To date, there have been few simulation studies of polymer collapse using models which employ an explicit solvent. The main reason is the huge computational cost of incorporating large numbers of solvent particles in the simulation. To overcome this problem, we have chosen to study a two-dimensional system in our first study on this topic,[36] and to study the properties of very short chains in three dimensions in the present study. The results are important: we now have a qualitative understanding of the effects of various generic system properties on the equilibrium properties and collapse dynamics for a model system that is a much better approximation to the dilute polymer solution considered theoretically and studied experimentally than the implicit-solvent systems previously considered. In addition the recent work of Chang and Yethiraj[37] has highlighted the fundamental qualitative difference in the collapse behavior between implicit-solvent and explicit-solvent systems.

On the other hand, the polymer chain lengths employed in the studies of Refs. 36 and 37, and especially in the present study, are still too low to test the quantitative predictions of many of the existing theories of polymer collapse. These theories typically predict a multistage collapse process, with collapse times that scale with chain length N in a very specific manner. The scaling exponents depend on, e.g., whether or not hydrodynamics has been built into the theory. Future simulation studies in this vein will have to employ considerably longer polymer chains, with a concomitant large increase the total number of particles. As well, other important features of the model system which should also be examined, such as the effect of varying the solvent/monomer particle size ratio, will also vastly increase the number of degrees of freedom, and thus the computational cost of the calculations. Of course, the ability to perform such large-scale simulations will improve with time as computers become faster and parallel-processing machines such as Beowulf clusters become more commonplace.

ACKNOWLEDGMENTS

The authors thank Christine Villeneuve for many stimulating discussions on polymer collapse dynamics. Financial support of the National Sciences and Engineering Research Council of Canada (NSERC) is acknowledged.

[1] W. H. Stockmayer, Macromol. Chem. Phys. **35**, 54 (1960).
[2] I. Nishio, S. T. Sun, G. Swislow, and T. Tanaka, Nature (London) **281**, 208 (1979).
[3] G. Swislow, S. T. Sun, I. Nishio, and T. Tanaka, Phys. Rev. Lett. **44**, 796 (1980).
[4] *Protein Folding*, edited by T. E. Creighton (Freeman, New York, 1994).
[5] E. I. Shaknovich, Curr. Opin. Struct. Biol. **7**, 29 (1997).
[6] V. S. Pande, A. Y. Grosberg, T. Tanaka, and D. S. Rokhsar, Curr. Opin. Struct. Biol. **8**, 68 (1998).
[7] P. G. de Gennes, *Scaling Concepts in Polymer Physics* (Cornell University Press, New York, 1979).
[8] F. Brochard, C. Williams, and H. L. Frisch, Annu. Rev. Phys. Chem. **32**, 433 (1981).
[9] A. Y. Grosberg and A. R. Khokhlov, *Statistical Mechanics of Macromolecules* (AIP, New York, 1994).
[10] P. G. de Gennes, J. Phys. (France) Lett. **46**, L639 (1985).
[11] A. Y. Grosberg, S. K. Nechaev, and E. I. Shakhnovich, J. Phys. (France) Lett. **49**, 2095 (1988).
[12] A. Halperin and P. M. Goldbart, Phys. Rev. E **61**, 565 (2000).
[13] L. I. Klushin, J. Chem. Phys. **108**, 7917 (1999).
[14] E. G. Timoshenko and K. A. Dawson, Phys. Rev. E **51**, 492 (1995).
[15] E. G. Timoshenko, Y. A. Kuznetsov, and K. A. Dawson, J. Chem. Phys. **102**, 1816 (1995).
[16] Y. A. Kuznetsov, E. G. Timoshenko, and K. A. Dawson, J. Chem. Phys. **104**, 3338 (1996).
[17] E. Pitard and H. Orland, Europhys. Lett. **41**, 467 (1998).
[18] E. Pitard, Eur. Phys. J. B **7**, 665 (1999).
[19] F. Ganazzoli, R. L. Ferla, and G. Allegra, Macromolecules **28**, 5285 (1995).
[20] Z. Wang, J. Yu, and B. Chu, Macromolecules **25**, 1618 (1992).
[21] Q. Ying, B. Chu, and A. Y. Grosberg, Macromolecules **28**, 180 (1995).
[22] P. W. Zhu and D. H. Napper, J. Chem. Phys. **106**, 6492 (1997).
[23] M. Nakata and T. Nakagawa, J. Chem. Phys. **110**, 2703 (1999).
[24] N. Kayaman, E. E. Gürel, B. M. Baysal, and F. E. Karasz, Macromolecules **32**, 8399 (1999).

[25] A. Y. Grosberg and D. V. Kuznetzov, Macromolecules **26**, 4249 (1993).
[26] E. G. Timoshenko, Y. A. Kuznetsov, and K. A. Dawson, Phys. Rev. E **54**, 4071 (1996).
[27] A. Byrne, P. Kierman, D. Green, and K. A. Dawson, J. Chem. Phys. **102**, 573 (1995).
[28] Y. A. Kuznetsov, E. G. Timoshenko, and K. A. Dawson, J. Chem. Phys. **103**, 4807 (1995).
[29] G. Tanaka and W. L. Mattice, Macromolecules **28**, 1049 (1995).
[30] B. Ostrovsky and Y. Bar-Yam, Europhys. Lett. **25**, 409 (1994).
[31] B. Ostrovsky and Y. Bar-Yam, Biophys. J. **68**, 1694 (1995).
[32] G. E. Crooks, B. Ostrovsky, and Y. Bar-Yam, Phys. Rev. E **60**, 4559 (1999).
[33] J. E. Straub, J. Ma, and E. I. Shakhnovich, J. Chem. Phys. **103**, 2615 (1995).
[34] H. S. Chan and K. A. Dill, J. Chem. Phys. **99**, 2116 (1993).
[35] G. C. Grayce, J. Chem. Phys. **106**, 5171 (1997).
[36] J. M. Polson and M. J. Zuckermann, J. Chem. Phys. **113**, 1283 (2000).
[37] R. Chang and A. Yethiraj, J. Chem. Phys. **114**, 7688 (2001).
[38] K. S. Schweizer and J. G. Curro, Adv. Polym. Sci. **116**, 1283 (1994).
[39] K. S. Schweizer and J. G. Curro, Adv. Chem. Phys. **98**, 1 (1997).
[40] M. P. Allen and D. J. Tildesley, *Computer Simulation of Liquids* (Clarendon, Oxford, 1987), pp. 149–152.
[41] G. J. Martyna, M. E. Tuckerman, D. J. Tobias, and M. L. Klein, Mol. Phys. **87**, 1117 (1996).
[42] M. Tuckerman, G. J. Martyna, and B. J. Berne, J. Chem. Phys. **93**, 1287 (1990).
[43] M. Tuckerman, B. J. Berne, and G. J. Martyna, J. Chem. Phys. **97**, 1990 (1992).
[44] Strictly speaking, the conserved quantity in NVT simulations employing the Nosé–Hoover thermostat is not the standard energy E, but rather a quantity with dimensions of energy, as described, e.g., in Ref. 41.
[45] D. Frenkel and A. A. Louis, Phys. Rev. Lett. **68**, 3363 (1992).
[46] M. Dijkstra and D. Frenkel, Phys. Rev. Lett. **72**, 298 (1994).
[47] M. Dijkstra, D. Frenkel, and J. P. Hansen, J. Chem. Phys. **101**, 3179 (1994).
[48] G. Luna-Bárcenas, G. E. Bennett, I. C. Sanchez, and K. P. Johnston, J. Chem. Phys. **104**, 9971 (1996).
[49] J. K. C. Suen, F. A. Escobedo, and J. J. de Pablo, J. Chem. Phys. **106**, 1288 (1997).
[50] P. G. Khalatur, L. V. Zherenkova, and A. R. Khokhlov, Eur. Phys. J. B **881**, 5 (1998).
[51] P. van der Schoot, Macromolecules **31**, 4635 (1998).
[52] J. M. Polson, Phys. Rev. E **60**, 3429 (1999).
[53] Strictly speaking, such a transition was observed in the study of Ref. 49. However, a collapse transition was observed only in the case where the solvent particle diameter was close to the radius of gyration of the polymer in the coil state. Such a model system more accurately describes a polymer–colloid mixture, rather than a polymer in solution.
[54] F. A. Escobedo and J. J. de Pablo, Mol. Phys. **89**, 1733 (1996).
[55] V. A. Ivanov, W. Paul, and K. Binder, J. Chem. Phys. **109**, 5659 (1998).
[56] Y. A. Kuznetsov and E. G. Timoshenko, J. Chem. Phys. **111**, 3744 (1999).
[57] V. A. Ivanov, W. Paul, and K. Binder, Macromol. Theory Simul. **9**, 488 (2000).
[58] H. Noguchi and K. Yoshikawa, J. Chem. Phys. **113**, 854 (2000).